Genetic-Algorithm Optimization of Birks' Law-based Response Functions for a Stilbene Scintillation Detector

Wonku Kim [a], Kilyoung Ko [a], Sunjin Kim [a], Jong-Bum Kim [a], Jin-Joo Kim [a], Deokseong Kim [a], Jintae Hong[a*]
[a]*Radioisotope Research Division, Korea Atomic Energy Research Institute,*
111, 989 beon-gil, Yuseong-gu Daejeon 34057, Republic of Korea
[*]*Corresponding author: jthong@kaeri.re.kr*

1. Introduction

Accurate characterization of neutron fields is essential in environments where neutron sources are present [1]. In practical settings, neutron energy distributions are readily altered by surrounding materials and shielding structures, and such spectral modifications can directly affect the reliability of dose assessment and radiation protection. Thus, a quantitative understanding of neutron radiation environments requires physically traceable modeling of detector responses, rather than reliance on simple count-rate or dose-based indicators alone.

Neutron detection using organic scintillation detectors is based on the energy deposition of recoil protons generated through elastic scattering between incident neutrons and hydrogen atoms. Recoil protons exhibit high linear energy transfer, leading to concentrated energy deposition over short track lengths. This localized energy deposition enhances interactions among excited states and increases non-radiative quenching processes, resulting in a nonlinear relationship between the deposited energy and the scintillation light output. Such nonlinearity is commonly described by Birks' law and represents a critical factor in the accurate modeling of neutron detector response functions. Accordingly, Birks' law-based physical modeling of the response function is an essential requirement for reliable neutron response characterization. However, in many previous studies, the nonlinear light-yield behavior described by Birks' law has been implicitly incorporated through empirical response tuning, limiting the explicit representation of detector physics within the response function [2-3].

In this study, we construct a neutron response function for an organic scintillation detector with the objective of ensuring physical consistency and robustness of the response function itself, without reliance on condition-specific empirical corrections. The nonlinear proton recoil light-yield behavior is explicitly incorporated into the response function through Birks' law in conjunction with a light-output resolution model, and the associated physical parameters are optimized using a global-search-based genetic algorithm (GA).

2. Materials and Methods

2.1 Experimental setup and overall analysis flow

Figure 1 illustrates the overall experimental setup and analysis workflow employed in this study. Neutron measurements were performed using a 1-inch stilbene organic scintillation detector coupled to a photomultiplier tube and a high-voltage supply. Detector signals were digitized using a fast waveform digitizer and recorded in a list-mode format for offline processing. Pulse shape discrimination (PSD) was applied to separate neutron-induced events from γ-ray background in a Python environment, and the resulting neutron light-output spectra were used as the primary experimental observables. Energy calibration of the detector was performed using standard γ-ray sources (^{22}Na, ^{137}Cs, and ^{60}Co) by identifying the corresponding Compton edges. Neutron sources (^{241}Am-Be and ^{252}Cf) were measured under identical detector and acquisition conditions. As summarized in Fig. 1, the overall analysis flow consists of experimental data acquisition, PSD, response-matrix optimization, and evaluation of detector response characteristics.

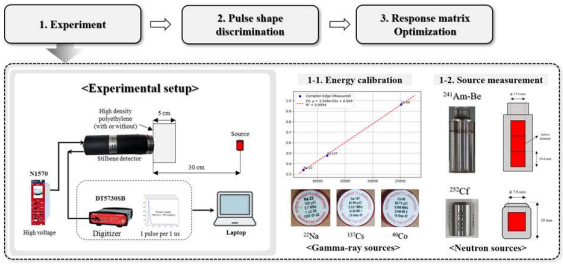

Fig. 1. Overview of the experimental setup and analysis flow.

2.2 Detector response modeling and genetic-algorithm-based optimization framework

Neutron detection in the stilbene scintillation detector is based on elastic scattering between incident neutrons and hydrogen nuclei, producing recoil protons that deposit energy in the scintillator. For an incident neutron energy E_n, the recoil proton energy distribution $P(E_p|E_n)$ was obtained using MCNP simulations. The scintillation light output $L(E_p)$ produced by a recoil proton of energy E_p was modeled using Birks' law,

$$L_{mean}(E_p) = \frac{AE_p}{1+BE_p}, \qquad (1)$$

where A represents the overall light output (L) scaling factor, and B accounts for the nonlinearity of the proton scintillation response [4]. The statistical spread of L is described by an energy-dependent resolution (σ_L) model expressed as a function of the mean light output:

$$\sigma_L^2(E_p) = a^2 L_{mean}(E_p) + b^2 L_{mean}(E_p)^2 + c^2 \qquad (2)$$

Using (1) and (2), the light-output response matrix $B(L|E_p)$ is constructed by assuming a Gaussian distribution of L for each E_p,

$$B(L|E_p) = \frac{1}{\sqrt{2\pi}\sigma_L(E_p)} exp\left[-\frac{(L-L_{mean}(E_p))^2}{2\sigma_L^2(E_p)}\right], \quad (3)$$

which was normalized along the L axis for each E_p. The probability of observing a light output for E_n, $R(L|E_n)$ is then obtained by combining $B(L|E_p)$ with $P(E_p|E_n)$, as defined in (4) and (5):

$$m_{pred}(L) = \sum_{E_p}\sum_{E_n} B(L|E_p)\,P(E_p|E_n)\phi(E_n)\Delta E_n\,, \quad (4)$$

$$R(L|E_n) = \sum_{E_p} B(L|E_p)\,P(E_p|E_n)\,, \quad (5)$$

where, $\phi(E_n)$ denotes the neutron flux spectrum. The parameters (A, B, a, b, c), including the Birks parameter and resolution coefficients, were optimized using a GA. The objective function ($\mathcal{L}$) was defined as Eq. (6) to minimize the discrepancy between the measured light-output spectrum $M(L)$ and the forward-calculated spectrum $C(L)$.

$$\mathcal{L} = \sum_L [M(L) - C(L)]^2 \quad (6)$$

In this study, the GA-based optimization framework was applied to three response cases defined by the neutron source data used for parameter optimization: R_1, optimized using a ^{241}Am-Be; R_2, optimized using a ^{252}Cf; and R_3, optimized using combined ^{241}Am-Be and ^{252}Cf. For all cases, the Birks' law parameters (A, B) and light-output resolution coefficients (a, b, c) were optimized under identical detector models and optimization settings, differing only in the reference neutron spectra.

3. Result and Discussion

3.1 PSD optimization results

Figure 2 shows the PSD scatter plots as a function of light output for the ^{241}Am-Be and ^{252}Cf sources obtained using the charge-comparison method. In both cases, neutron and γ-ray events form clearly separated band structures over the full light-output range. Neutron-induced events exhibit systematically higher PSD ratios than γ-ray events. Despite differences in the neutron emission characteristics of the two sources, stable neutron–γ discrimination was achieved using the same energy-dependent separation curve. In the following analysis, only events classified as neutrons were selected and used to construct the measured light-output spectra for response function optimization.

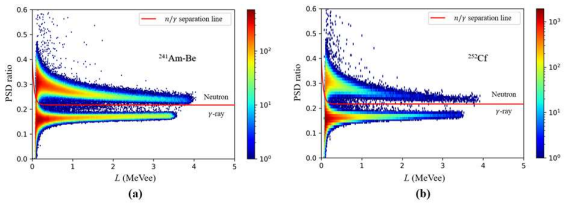

Fig. 2. PSD scatter plots showing neutron-γ separation using the charge comparison method for (a) ^{241}Am-Be and (b) ^{252}Cf.

3.2 Parameter optimization results

Table 1 lists the Birks' law and light-output resolution parameters optimized for the three response cases (R1–R3) using the GA-based framework. All cases converged stably to physically reasonable parameter sets, indicating that the nonlinear proton recoil light-yield behavior was consistently captured regardless of the neutron source data used during optimization. While moderate variations in the optimized parameters were observed among R1–R3, these differences primarily reflected the spectral characteristics of the reference neutron sources rather than changes in the underlying detector response.

Table 1. Optimized Birks' law and energy resolution parameters.

	Response matrix ID		
	R_1	**R_2**	**R_3**
A	0.2267	0.2102	0.2500
B	0.0078	0.0114	0.0079
a	0.0521	0.0369	0.0396
b	2.5504	0.5130	0.6954
c	0.1021	0.0653	0.0334

To quantitatively compare the optimized response matrices, the relative difference $\Delta R_{rel}(L|E_n)$ with respect to the reference matrix R_1 was defined as:

$$\Delta R_{rel}(L|E_n) = \frac{R_n(L|E_n) - R_1(L|E_n)}{R_1(L|E_n)} \text{ (n = 2, 3)}, \quad (7)$$

Figure 3 shows the relative difference maps for ΔR_2 and ΔR_3. For both cases, the overall response-matrix structures were consistent with that of R_1, with noticeable deviations confined to limited regions of low response probability. Compared with R_2, the response matrix optimized using combined source data (R_3) showed reduced localized differences.

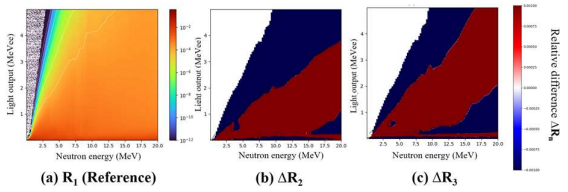

Fig. 3. Reference response matrix and relative difference maps for different calibration scenarios.

Figure 4 compares the light-output spectra predicted using the optimized response matrices (R_1–R_3) with the reference spectra derived from MCNP neutron flux distributions for the ^{241}Am-Be and ^{252}Cf sources. For both sources, the response matrix optimized using combined source data (R_3) provided consistently good agreement with the MCNP-based spectra over the full light-output range, demonstrating robust predictive performance across different neutron fields. The source-specific response matrices (R_1 and R_2) also reproduce the overall spectral trends, with R_2 showing minor deviations at higher light-output regions. These deviations are attributed to small differences between the measured and MCNP-simulated neutron spectra and remained limited in magnitude.

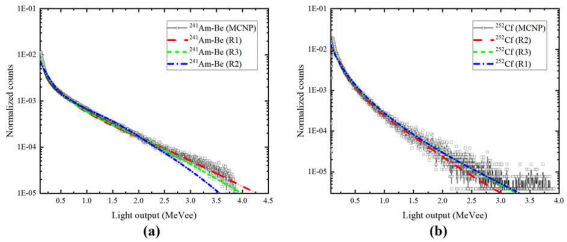

Fig. 4. Forward-calculated light-output spectra using unfolded neutron fluxes for (a) ^{241}Am-Be and (b) ^{252}Cf.

4. Conclusion

In this study, a Birks' law-based neutron response function for a stilbene scintillation detector was developed using a genetic-algorithm-based optimization framework. The optimized response matrices showed physically consistent behavior and robust predictive performance across different neutron sources. Future work will extend this framework to neutron spectrum unfolding and dose evaluation for radiation protection applications.

ACKNOWLEDGEMENT

This work was supported by Korea Research Institute for defense Technology planning and advancement (KRIT) grant funded by the Korea government (DAPA, Defense Acquisition Program Administration) (22-107-C00-007) (JRIT-CT-23-055).

REFERENCES

[1] R. M. Ambrosi et al., "European radioisotope thermoelectric generators (RTGs) and radioisotope heater units (RHUs) for space science and exploration," Space Science Reviews, vol. 215, no. 55, 2019.
[2] V. Suman and P. K. Sarkar, "Neutron spectrum unfolding using genetic algorithm in a Monte Carlo simulation," Nuclear Instruments and Methods in Physics Research Section A, vol. 737, pp. 76–86, 2014.
[3] H. Shahabinejad, S.A. Hosseini, M. Sohrabpour, "A new neutron energy spectrum unfolding code using a two-step genetic algorithm," Nuclear Instruments and Methods in Physics Research Section A, vol. 811, pp. 82–93, 2016.
[4] J. B. Birks, The Theory and Practice of Scintillation Counting. Oxford, U.K.: Pergamon Press, 1964.